

# Gluon vs. quark fragmentation – from LEP to FCC-ee

Klaus Hamacher<sup>1</sup>

<sup>1</sup>Bergische U. Wuppertal, Germany

**Abstract:** Experimental results on gluon and quark fragmentation obtained by the LEP experiments are reviewed. The importance of colour coherence, transverse-momentum-scales and hadronisation corrections for jet measurements is emphasized. Precision results on multiplicities of three-jet events and the deduced multiplicity of a gluon-gluon colour neutral system are discussed. Identified particle results and colour octet neutralisation are addressed. Prospects for corresponding measurements at the FCC-ee are given.

## Introduction

At the time of LEP several topics of strong interaction physics were still incompletely understood. Many questions could be clarified in the very clean  $e^+e^-$  environment with unprecedented statistical precision. Among those were basic predictions concerning the comparison of gluon and quark fragmentation. Such a comparison is attractive as the different colour structure of gluons and quarks should be immediately evident. In this talk I briefly review the basic experimental strategies. Then results for gluon and quark jets and the limitations of such measurements are discussed before coming to precision results on the multiplicity in three-jet events. Finally some results on identified particles and open topics on octet neutralisation are discussed before giving the outlook to FCC-ee.

## Basic Ideas and Experimental Strategy

In the hadronic final state of  $e^+e^-$  annihilation, gluon and quark fragmentation can be compared in events with three jets, two of which originate from the initially produced  $q\bar{q}$  pair, the third from a radiated hard gluon. The mutual assignment of partons to jets is done at tree-level, thereby limiting the quantitative comparison of gluon and quark jet properties to leading order precision. This basic limitation can only be overcome when studying more inclusive properties of three-jet events, like the event multiplicity or overall particle spectra. Still even then the identification of jets introduces some systematic dependence on the jet algorithm chosen. Moreover, the parton properties underlying a three-jet event need to be determined from the observed jets. This implies that hadronisation needs to be considered when determining the parton properties! This inevitably introduces bias and smearing which may strongly influence e.g. observed fragmentation functions. Experimentally gluon jets are enriched using energy ordering and anti-tagged by identifying heavy hadron decays predominantly in b quark events. Gluon jets are then compared to a mixture of light quark and gluon jets in, again, anti-tagged light quark events or to events where the gluon is replaced by an isolated photon. The kinematics in these events is chosen similar to those containing the tagged gluons. The respective purities of gluon and quark jets are taken from simulation, pure gluon and quark distributions are inferred using matrix inversion.

Initially these techniques were applied to the so called Y-events [1,2,3,4], containing two jets with similar energy ( $E \lesssim 25$  GeV) and angle with respect to the event axis. Also fully symmetric ("Mercedes"-star) events [5,6] and events where a gluon jet recoils with respect to two quark jets [7,8] were used, again comparing to properties of jets of similar energy. After recognising that

Table 1: Selected data on the hadron multiplicity ratio in gluon to quark jets as a function of jet energy.

Exp.	$E_{Jet}/\text{GeV}$	$r_n$
Cleo	[12]	3.5
HRS	[13]	9.7
Aleph	[14]	24
Delphi	[5]	24
Opal	[7]	40

the energy is an inappropriate scale, as it depends on the Lorentz-system [9], invariant transverse-momentum-scales have been introduced. The above technique was then expanded to general three-jet topologies. This allowed gluon to quark comparisons in a large kinematic range [10].

## Initial Results on Jet Fragmentation

It is a basic QCD expectation that the hadron multiplicity is proportional to the colour charge of the radiating parton [11], i.e. the multiplicity ratio in gluon to quark jets should be  $C_A/C_F = 9/4 = 2.25$ . The experimentally seen ratio is far smaller (see Table 1), however, indicates a clear increase with energy [5].

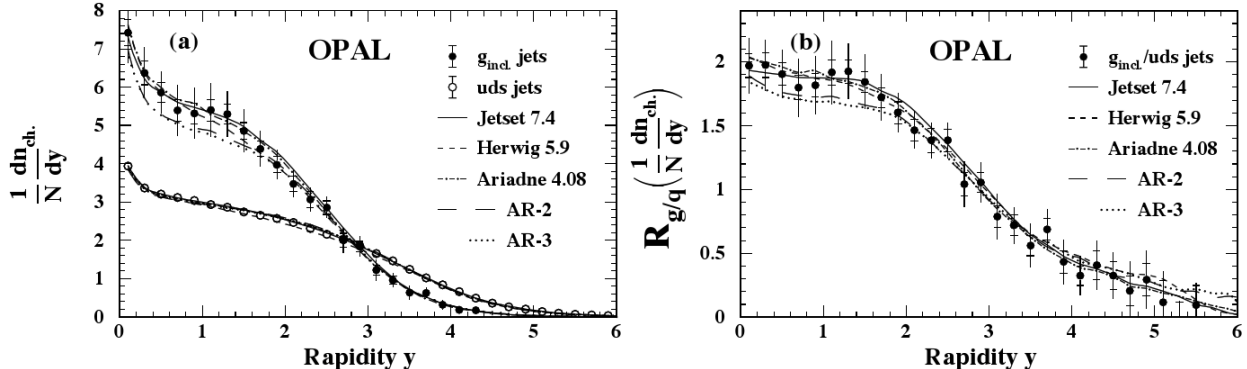


Figure 1: Rapidity-distribution for gluon & quark jets (left) and their ratio (right) [15].

The small multiplicity can be understood by inspecting the rapidity (or  $y$ ) distribution of the produced particles with respect to the event axis (see Figure 1). Here the gluon distribution is taken from events where the gluon recoils with respect to two b-jets. The average gluon energy is  $E_g = 40\text{GeV}$ , the transverse momentum with respect to the quark-jets  $\kappa_g \sim 37\text{GeV}$ . The quark distribution stems from light quark events with  $E_q = \kappa_q = 45.6\text{GeV}$  [7].

At small  $y$ , that is for particles produced first in time [17], the production rate is a factor  $\lesssim 2$  higher for gluons compared to quarks. For  $y \gtrsim 2$  the ratio falls off strongly and for  $y > 3$  more particles are produced in quark compared to gluon jets. The latter to a large part is a consequence of energy conservation; there is not enough energy left in gluon jets to produce additional particles.

Moreover, particle production in quark jets may be eased as quarks are valence particles of hadrons. Overall this extra production diminishes the total multiplicity ratio. Still, even at small rapidity the expectation 2.25 is not met. This partly is due the difference in the relevant scales ( $E_q, \kappa_g, \sim 20\%$ ) of the underlying partons, but also affected by coherent emission from the underlying  $q\bar{q}g$ -ensemble and the expected destructive interference (the so-called string effect, see next section).

In order to illustrate the evolution of the parton multiplicity the so-called subjet-rates  $R_i$  and their derivatives have been compared for gluon and quark jets [16].  $R_1$  is the experimental equivalent to the Sudakov form factor  $\Delta(y)$  (see e.g. [18]):

$$\begin{aligned} \Delta(y|y_0) &= \exp \left\{ - \int_{y_0}^y \Gamma_{p \rightarrow p'p''}(y') dy' \right\} \stackrel{!}{=} R_1(y) = \frac{N_1(y)}{N_0} \\ -\Gamma(y) &= \tilde{D}_1(y) = \frac{1}{N_1(y)} \frac{\Delta N_1(y)}{\Delta y} \\ \Gamma_q(y, y_0) &= \frac{C_F \alpha_s}{2\pi} \left( \ln \frac{y}{y_0} - \frac{3}{2} \right) \quad \Gamma_g(y, y_0) = \frac{C_A \alpha_s}{2\pi} \left( \ln \frac{y}{y_0} - \frac{11}{6} \right) \end{aligned} \quad (1)$$

$R_1(y)$  is the 1-jet rate, which is the probability, that at a given resolution,  $y$ , no splitting has happened in a jet, i.e. there is still only 1 "parton" present.  $\Gamma_p(y)$  is the probability density for a parton  $p = (q, g)$  to split at a given  $y$ ,  $\tilde{D}_1$  is the corresponding experimental observable.  $D_1(y) = R_1(y) \cdot \tilde{D}_1(y)$  is the rate of parton splitting. This concept has been generalised for higher rank ( $2 \rightarrow 3, 3 \rightarrow 4 \dots$ ) splittings [16,19].

A measurement of the splitting kernels (multiplied by  $y$ ) is shown in Figure 2. The splitting probability ( $\tilde{D}_1$ ) is markedly bigger for gluon compared to quark jets at high  $y$ . Deviations from the NLLA expectations  $\Gamma_p$  (see Equation 1) due to hadronisation set in at higher  $y$  for gluons compared to quarks. The ratio  $r_1 = \tilde{D}_1^g / \tilde{D}_1^q$  for large  $y$  is initially close to  $C_A/C_F$ , but showing a hump-structure which is described by fragmentation models (see Figure 2). Most likely the hump is a consequence of hadronisation smearing. Such a structure would be expected, as the splitting kernels are strongly varying functions of  $y$  below a maximal value of  $y_0 \sim 1/3$ .

Figure 3 shows the related jet and splitting rates and splitting probabilities for the first four splittings. The rates  $R_i$  show a well known pattern from multi jet rates in  $e^+e^-$  (in this case one usually starts from the initial 2 jets). The splitting rates  $D_i$  are far higher at higher  $y$  for gluons, but for each rank this initial lead is compensated at smaller  $y$  in quark jets. The splitting probability  $\tilde{D}_i$ , which for the first rank  $i = 1$  splitting is about two times higher for gluons, converges to similar values for the gluon and quark cases at higher rank splittings. This general pattern easily explains the observed small gluon to quark hadron multiplicity ratio.

Especially the gluon fragmentation function(s)  $D_g^h(z)$  to a hadron  $h$  is a quantity which was intensively studied at LEP in  $e^+e^-$  three-jet events. Initial measurements were done for Y- and Mercedes-events [3,4,16] and later extended to more general topologies [10,20,21]. Also boosting to symmetric topologies was used in order to ease the assignment of hadrons to partons [22]. In view of the studies of the scale dependence of the gluon and quark fragmentation functions, the introduction of transverse-momentum-like scales was an important step [10,19,23]. Relevant scales are:

$$\text{quark: } \kappa = E_q \sin \frac{\Theta_{qg}}{2} \quad \text{gluon: } p_\perp = \frac{1}{2} \sqrt{\frac{s_{qg} s_{\bar{q}g}}{s_{e^+e^-}}} \quad . \quad (2)$$

Here,  $\Theta_{qg}$  is the angle between the gluon and the closest quark jet and  $s$  is the Mandelstam variable. Essentially  $p_\perp$  is the harmonic mean of the transverse momenta of the gluon with respect to quark

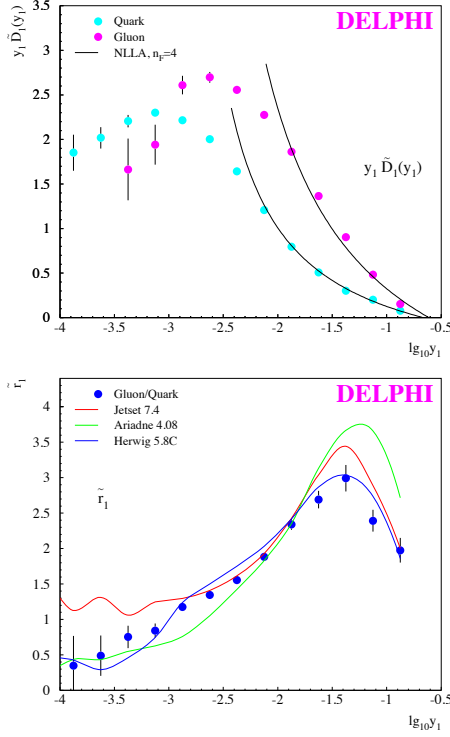


Figure 2: gluon & quark splitting kernels compared to the NLLA expectation (up) and their ratio compared to MC models (down) [16]. NLLA predicts  $r_1 = 2.25$  ( $n_f = 3$ ).

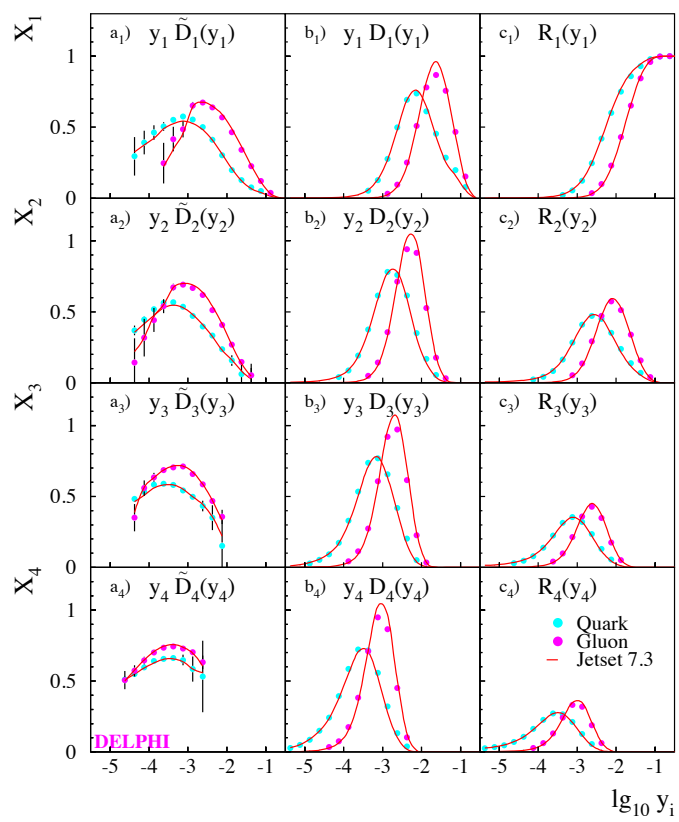


Figure 3: Gluon and quark subjet-rates ( $R_i$ ), splitting-rates ( $D_i$ ) and splitting probabilities/kernels  $\tilde{D}_i$  compared to MC models [16].

or anti-quark, respectively. These scales, as well as the parton energy  $E_p$  used in the denominator of the scaling variable  $x_E \sim z = E_{had}/E_p$  need to be determined from the jet properties, therefore, they acquire experimental as well as hadronisation uncertainties.

The measured fragmentation function for quarks agrees well with the corresponding results from  $e^+e^-$  at lower energies (see Figure 4 [21]) as well as with DGLAP fits. The corresponding gluon result is shown in Figure 5 and shows the expected stronger fall-off with  $z \sim x_E$  as well as with the scale ( $p_\perp$ ) compared to quarks. The ratio of the logarithmic slopes of the gluon and quark-fragmentation functions was the first measurement which quantitatively verified the colour factor ratio from a gluon measurement [10]:  $C_A/C_F = 2.26 \pm 0.09 \pm 0.14$ .

From a comparison of the data at high  $x$  and the DGLAP fits it is obvious that the slope of the data exceeds that of the fits. This is a consequence of the irreducible smearing due to hadronisation and the corresponding uncertainty of the measured properties (momentum or energy  $E_p$ ) of the partons in the event [24]. This uncertainty can be analytically estimated using the longitudinal phase space or tube model (see e.g. [18]) to be of the order  $0.5\text{GeV}/E$ . Applying this smearing to an analytic approximation of the data (taken from [10]) explains the observed deviation between the DGLAP fits (lower curves in Figure 6) and the data (represented by the upper curves). Due to the stronger fall-off of the fragmentation function with  $z$  or  $x$  for gluons the effect is here far more pronounced as for quarks. This basic problem inevitably appears whenever parton properties are measured from data. It is particularly big at small jet energy and for rapidly varying distributions

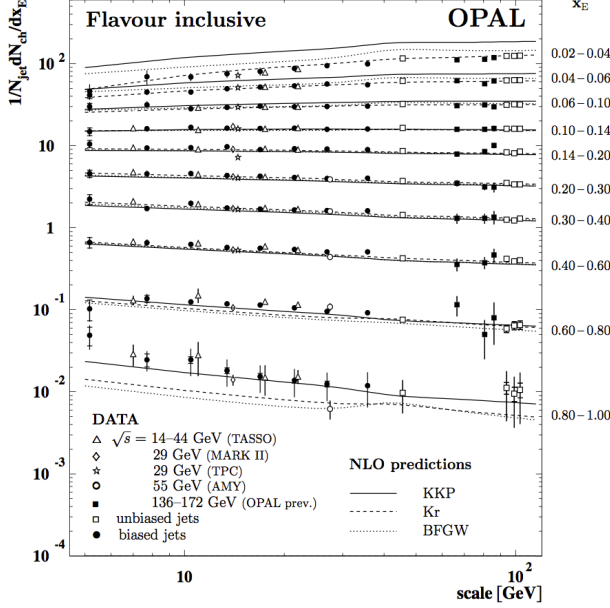


Figure 4: Quark fragmentation function as measured from three-jet events [21].

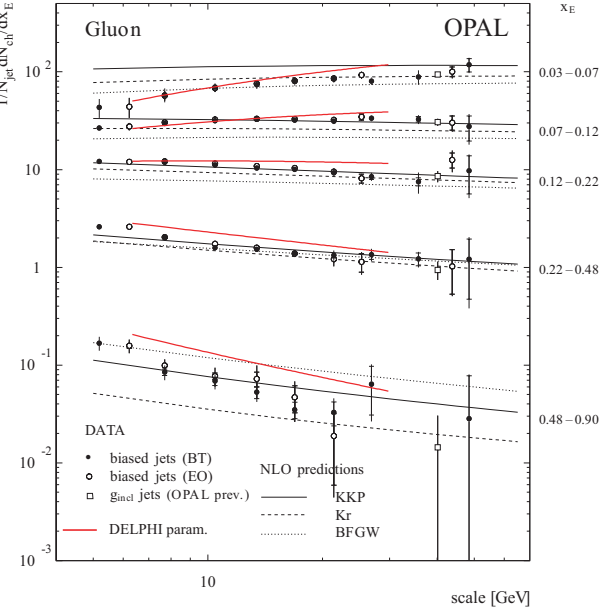


Figure 5: Gluon fragmentation function corresponding to Figure 4. The additional line represents a parameterisation of the data from [10].

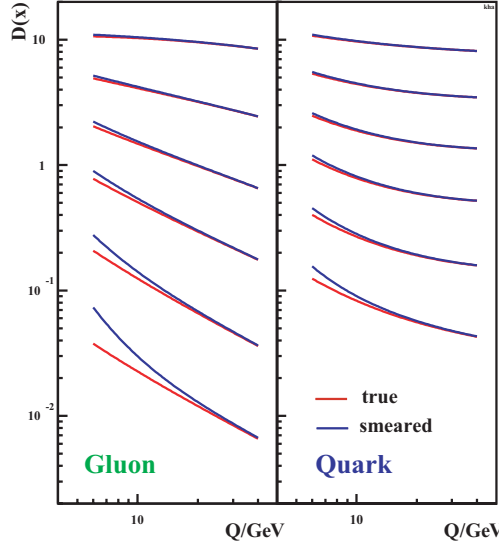


Figure 6: Effect of the hadronisation smearing of the parton properties on the fragmentation functions measured in three-jet events. The lower curves represent the true distributions, the upper curves the measured distributions.

\*!

\*Using error propagation the E-uncertainty is to be multiplied by the relative slope of the distribution.

## Multiplicity in Three-Jet Events

Coherent emission of hadrons from a  $q\bar{q}g$ -ensemble can be best observed using soft, low resolution, large wavelength hadrons emitted at large angles with respect to the underlying partonic system. A parameter free prediction for the ratio of particle rates produced perpendicular to the event plane of a three-jet event and the event axis in a  $q\bar{q}$ -event reads [25]:

$$\frac{N_{\perp}^{q\bar{q}g}}{N_{\perp}^{q\bar{q}}} = \frac{C_A}{C_F} \cdot r_t = \underbrace{\frac{C_A}{C_F}}_{\text{colour factor}} \cdot \frac{1}{4} \left[ \widehat{q}g + \widehat{\bar{q}}g - \underbrace{\frac{1}{N_C^2} \widehat{q}\bar{q}}_{\text{destructive interf.}} \right] , \quad (3)$$

with the number of colours  $N_C = 3$  and (note the correspondence to Equation 2):

$$\widehat{i}j = 2 \sin^2 \frac{\Theta_{ij}}{2} .$$

The destructive interference term represents the so called "string effect" [17] for this special kinematic situation. Note, that expression 3 is linear in the colour factor ratio and in the topological term  $r_t$ . For  $r_t \sim 1$  the gluon and a quark jet are close by, the relevant colour charge is that of the initial quark. For large  $r_t \rightarrow 2$  the gluon recoils with respect to the  $q\bar{q}$  pair. The radiating colour charge then corresponds to two quark charges.

Experimentally expression 3 is studied [26,27] using two- and three-jet events selected using  $k_t$ -type jet algorithms with fixed  $y_{cut}$ . Events with more than three jets were discarded. Particle rates are measured in cones of  $\sim 30^\circ$  opening angle. The resulting ratio (see Figure 7) is insensitive with respect to variations of  $y_{cut}$  and cone opening-angle.

The theoretical prediction given by Equation 3, including the destructive interference term, agrees well with the data for a large range of arbitrary and symmetric three-jet topologies. Exploiting the strictly linear  $r_t$ -dependence, the colour factor ratio can be extracted fitting the middle term of Equation 3 to the data (see Figure 8):

$$C_A/C_F = 2.211 \pm 0.014_{(\text{stat.})} \pm 0.045_{(\text{sys.})} .$$

The systematic uncertainty enfolds a variation of the cone angle between  $20^\circ$  and  $40^\circ$  and a variation of  $y_{cut}$  by a factor 2.

When measuring multiplicity the assignment of particles to jets imposes an obvious difficulty. Therefore, precision measurements rely on the overall multiplicity of three-jet events. A prediction for this multiplicity reads [17,28,29]:

$$N_{q\bar{q}g}(L_{q\bar{q}}, \kappa_{Lu}, \kappa_{Le}) = N_{q\bar{q}}(L_{q\bar{q}}, \kappa_{Lu}) + \frac{1}{2} N_{gg}(\kappa_{Le}) \quad (4)$$

$$L_{q\bar{q}} = \ln \left( \frac{s_{q\bar{q}}}{\Lambda^2} \right), \quad \kappa_{Lu} = \ln \left( \frac{s_{qg}s_{\bar{q}g}}{s\Lambda^2} \right), \quad \kappa_{Le} = \ln \left( \frac{s_{qg}s_{\bar{q}g}}{s_{q\bar{q}}\Lambda^2} \right)$$

This prediction takes coherence effects as well as the reduction of phase-space for gluon emissions from the quarks due to the emission of the leading gluon into account by the choice of scales. The

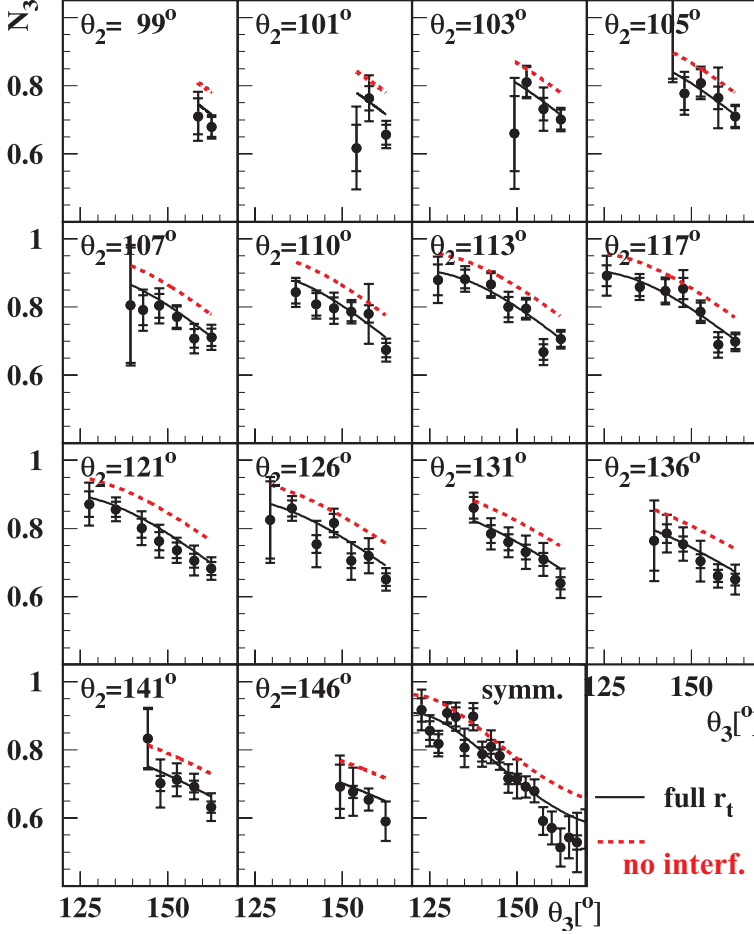


Figure 7: Ratio of particle production in  $30^\circ$  cones perpendicular to the event plane of three-jet events and the event axis of two-jet events [26]. The full line represents the parameter free prediction 3, for the dashed line destructive interference is omitted.

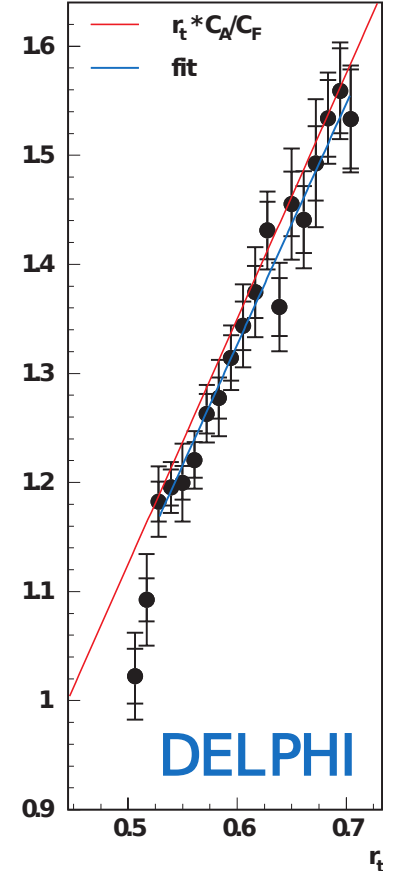


Figure 8: Data as in Figure 7, however, as function of  $r_t$ . The upper line is the expectation Equation 3, the lower line a fit to the data.

sub-division of the multiplicity in a quark- ( $N_{q\bar{q}}$ ) and a gluon part ( $N_{gg}$ ) is motivated by the case when a photon replaces the gluon. An alternative choice assigning less multiplicity to the gluon is possible [28].

It has been observed experimentally [30] that the small gluon to quark multiplicity ratio is largely due to a non-perturbative offset (clearly evident from the almost equal gluon and quark multiplicity at small energy, see Table 1) and that it is more efficient to determine the colour factor ratio from the ratio of the energy slopes of the multiplicities. Asymptotically this ratio is identical to the multiplicity ratio because of de l'Hôpital's rule. In the dipole model the energy slope of the gluon and quark multiplicity is connected by the differential equation [28]:

$$\left. \frac{dN_{gg}(L')}{dL'} \right|_{L'=L+c_g-c_q} = \frac{C_A}{C_F} \left( 1 - \frac{\alpha_0 c_r}{L} \right) \frac{d}{dL} N_{q\bar{q}}(L) \quad (5)$$

$\alpha_0 c_r$  are known constants.  $N_{q\bar{q}}(E)$  is known from  $e^+e^-$  experiments. The solution of Equation 5 leaves a constant of integration free, which allows to accommodate non-perturbative differences

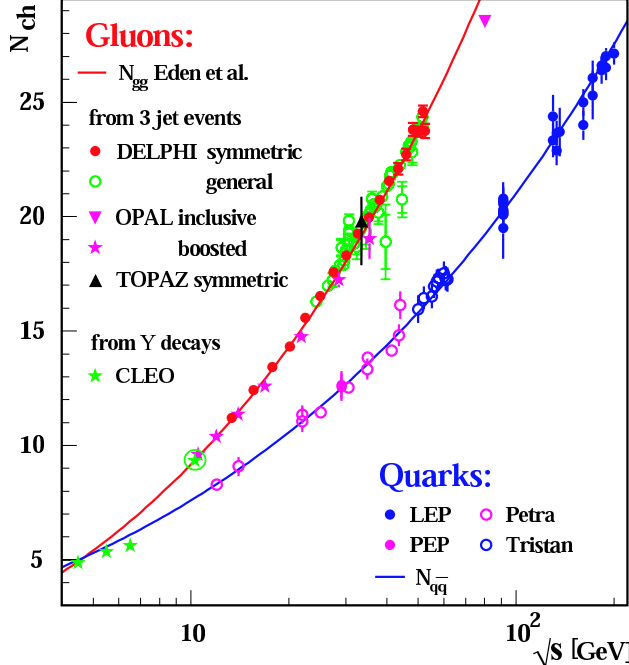


Figure 9: Hadron multiplicity in  $e^+e^-$  annihilation and corresponding result for a colour singlet gluon pair [12] deduced from three-jet multiplicity measurements [6,7,22,31].

between the gluon and the quark multiplicity.

The three-jet multiplicity has been measured by several experiments [15,20,22,30,31] including related  $p\bar{p}$ -results [32]. Fitting the dipole prediction to symmetric and arbitrary three-jet topologies while leaving the offset floating, leads to a precise result for the colour factor ratio,

$$\frac{C_A}{C_F} = 2.261 \pm 0.014_{\text{stat.}} \pm 0.036_{\text{exp.}} \pm 0.052_{\text{theo.}} \pm 0.041_{\text{clus.}} , \quad (6)$$

from the multiplicity slopes [31]. From a comparison of symmetric and arbitrary topologies it turned out that the alternative choice of scales (see [28] used in [15]) is unable to describe the full dataset.

Equation 4 can be solved for  $N_{gg}$ , the hadron multiplicity of a colour neutral gluon pair, shown in Figure 9. Note that the results obtained from three-jet events are well consistent with the only available direct  $N_{gg}$  result so far from  $\chi_b$ -decays [12]. The gluon to quark colour factor ratio is immediately evident from the different energy slopes in this figure.

Essential outcome of the studies discussed so far is:

- It is important to use the correct transverse-momentum-like scales which reflect the colour structure of the events. When inferring parton properties from jets, hadronisation effects should be considered.
- The influence of non-perturbative and finite-energy effects on gluon jets is stronger than for quark jets.
- Basic QCD properties can be more easily observed from dynamical variations of gluon and quark observables with the relevant scales.

## Identified Particles and Colour Octet Neutralisation

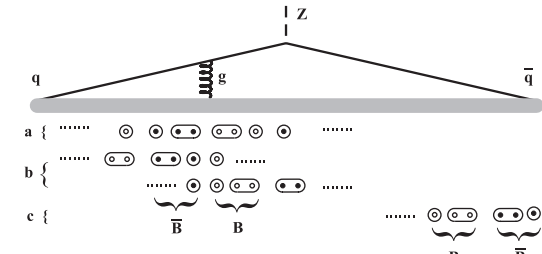
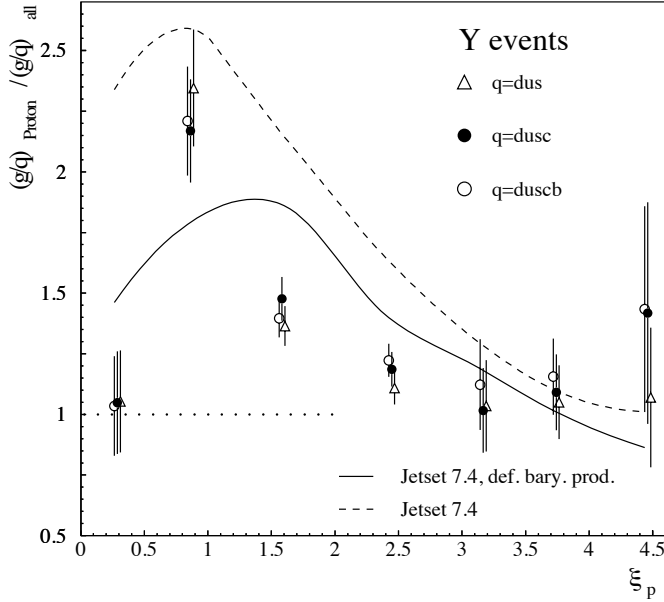


Figure 10: Chances for di-quark production in gluon (a,b) and quark jets (c) in the string model (up). Ratio of proton-production in gluon to quark jets normalised to the charged multiplicity ratio (left) [42].

Measurements of identified particle production have been performed at LEP in order to reveal possible differences in gluon and quark fragmentation. Hadronisation happens via an intermediate parton shower, which is by far dominated by gluons due to the structure of the splitting kernels. Differences are mainly expected for leading particles. For gluons there should be extra production of leading isoscalar particles [33,34,35,36] due to octet colour neutralisation (see Figure 11). Experimentally, no extra production of such states ( $\Phi, \eta, \eta'$ ) could be observed so far at LEP [19,37,38,39]. There is however increased baryon production in gluon jets [38,40,41,42] as well as in  $\Upsilon$ -decays via gluons [43]. At LEP the extra production is focussed at small  $\xi_p = -\ln x$ , thus large  $x$ , see Figure 10. Here the double ratio of proton to hadron production is shown for gluon and quark jets in order to eliminate the general difference due to the colour factors. The excess at  $\xi_p \sim 0.8$  can be understood in the string model [44]. Here an additional possibility for a splitting into a diquark anti-diquark pair exists (see Figure 10 case a), which via the Golden Rule leads to extra baryon production. This possibility is not present in cluster fragmentation.

In order to more generally search for isoscalar states, which are presumed to be heavy and for kinematic reasons must show a correspondingly hard fragmentation, it has been suggested to look for neutral leading systems with a rapidity gap [36]. The measurements [8,46,47] indeed indicate a small excess  $\sim 2\%$  of leading neutral systems in gluon jets (see Figure 11). It has, however, so far not been possible to clarify this excess in detail. From the mass spectra there is an indication for an excess at masses  $\lesssim 2\text{GeV}$ .

In [48] deviations of the overall momentum spectra for gluons have been reported, while the quark spectra are perfectly described by the tuned MC models. The deviation starts in the model to data ratio at  $x \sim 0.2$  and increases to about  $-30\%$  at very high  $x$ . As the comparison has been done with fully simulated events, no hadronisation smearing enters. Overall the size of the effect amounts to about the same size as that observed for leading neutral systems.

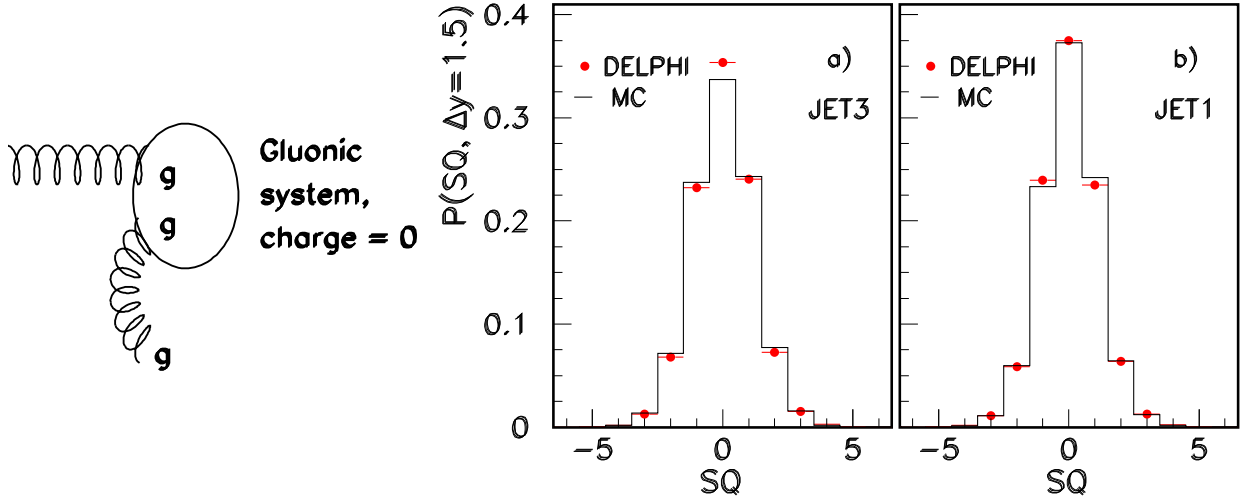


Figure 11: Octet neutralisation (left). Fraction of leading systems with charge  $SQ$  in gluon (a) and quark (b) jets. Lines are a prediction of Ariadne [45] .

### Outlook to FCC-ee

FCC-ee will provide an enormous number of events exceeding the total statistics at LEP between 40GeV (accessible by radiative events) and 240GeV, even at 350GeV almost the LEP statistics is reached. About  $10^{10}$  tagged three-jet events shall be provided at the Z. For gluon to quark comparisons this should allow to study "any" dynamical dependence (fragmentation functions, splitting kernels ...) with a negligible statistical uncertainty. Systematics can be largely mitigated by unfolding and controlled using the energy dependence. The topology dependence can be explicitly compared to the energy dependence.

Deep understanding of gluon and quark jets (like for the differing width) will influence many other important measurements, e.g.  $h \rightarrow gg$ , which itself is a testing bed for  $gg$  colour singlet fragmentation.

The high statistic will allow for studies of rare or difficult to measure processes. Leading particles in gluon and quark jets can be compared in order to search for octet fragmentation in jets, isoscalars and glueballs. Detailed studies and comparisons of mass plots will become possible and allow to search for meson as well as baryon resonances ( $\Delta, \Lambda(1520), \dots$ ). Additional questions will, in the meanwhile, be raised by low energy and lattice results.

For an FCC-ee experiment a high resolution electromagnetic calorimetry as well as very good particle identification and tracking are desirable. These should allow optimal determination of the jets as well as measurements of identified (neutral) particles and resonances.

## References

- [1] G. Alexander *et al.* [OPAL], Phys. Lett. B **265** (1991) 462.
- [2] P. D. Acton *et al.* [OPAL], Z. Phys. C **58** (1993) 387.
- [3] R. Akers *et al.* [OPAL], Z. Phys. C **68** (1995) 179.
- [4] D. Buskulic *et al.* [ALEPH], Phys. Lett. B **384** (1996) 353.
- [5] P. Abreu *et al.* [DELPHI], Z. Phys. C **70** (1996) 179.
- [6] K. Nakabayashi *et al.* [TOPAZ], Phys. Lett. B **413** (1997) 447.
- [7] G. Abbiendi *et al.* [OPAL], Eur. Phys. J. C **11** (1999) 217 [hep-ex/9903027].
- [8] G. Abbiendi *et al.* [OPAL], Eur. Phys. J. C **35** (2004) 293 [hep-ex/0306021].
- [9] G. S. Japaridze, Z. Phys. C **32** (1986) 59.
- [10] P. Abreu *et al.* [DELPHI], Eur. Phys. J. C **13** (2000) 573.
- [11] S. J. Brodsky and J. F. Gunion, Phys. Rev. Lett. **37** (1976) 402.
- [12] M. S. Alam *et al.* [CLEO], Phys. Rev. D **46** (1992) 4822.
- [13] M. Derrick *et al.*, Phys. Lett. **165B** (1985) 449.
- [14] D. Buskulic *et al.* [ALEPH], Phys. Lett. B **346** (1995) 389.
- [15] G. Abbiendi *et al.* [OPAL], Eur. Phys. J. C **23** (2002) 597 [hep-ex/0111013].
- [16] P. Abreu *et al.* [DELPHI], Eur. Phys. J. C **4** (1998) 1.
- [17] Y. L. Dokshitzer, V. A. Khoze, A. H. Mueller and S. I. Troian, “Basics of perturbative QCD,” Gif-sur-Yvette, France: Ed. Frontieres (1991) 274 p. (Basics of)
- [18] R. K. Ellis, W. J. Stirling and B. R. Webber, “QCD and collider physics,” Camb. Monogr. Part. Phys. Nucl. Phys. Cosmol. **8** (1996) 1.
- [19] O. Klapp, “Eine umfassende Studie der Eigenschaften von Gluon- und Quark-Jets,” WUB-DIS-99-16.
- [20] R. Barate *et al.* [ALEPH], Z. Phys. C **76** (1997) 191.
- [21] G. Abbiendi *et al.* [OPAL], Eur. Phys. J. C **37** (2004) no.1, 25 [hep-ex/0404026].
- [22] G. Abbiendi *et al.* [OPAL], Phys. Rev. D **69** (2004) 032002 [hep-ex/0310048].
- [23] M. Siebel, ”Fragmentationsfunktionen von Quarks und Gluonen - eine Untersuchung der Skalenverletzung in und der Multiplizitaet von Quark- und Gluon-Jets”, Diplomarbeit, BU-Gh Wuppertal WU D 97-43.
- [24] K. Hamacher, Acta Phys. Polon. B **36** (2005) 433.
- [25] V. A. Khoze, S. Lupia and W. Ochs, Eur. Phys. J. C **5** (1998) 77 [hep-ph/9711392].

- [26] J. Abdallah *et al.* [DELPHI], Phys. Lett. B **605** (2005) 37 [hep-ex/0410075].
- [27] M. Siebel, “Kohärente Teilchenproduktion in Dreijetereignissen der  $e^+e^-$ -Annihilation : Eine Untersuchung der Multiplizität in Quark-Gluon-Ensembles und eine präzise Bestimmung von  $C_A/C_F$  mit Daten des DELPHI-Experimentes,” WUB-DIS-2003-11.
- [28] P. Eden and G. Gustafson, JHEP **9809** (1998) 015 [hep-ph/9805228].
- [29] P. Eden, G. Gustafson and V. A. Khoze, Eur. Phys. J. C **11** (1999) 345 [hep-ph/9904455].
- [30] P. Abreu *et al.* [DELPHI], Phys. Lett. B **449** (1999) 383 [hep-ex/9903073].
- [31] J. Abdallah *et al.* [DELPHI], Eur. Phys. J. C **44** (2005) 311 [hep-ex/0510025].
- [32] D. Acosta *et al.* [CDF], Phys. Rev. Lett. **94** (2005) 171802.
- [33] I. Montvay, Phys. Lett. **84B** (1979) 331.
- [34] C. Peterson and T. F. Walsh, Phys. Lett. **91B** (1980) 455.
- [35] H. Spiesberger and P. M. Zerwas, Phys. Lett. B **481** (2000) 236 [hep-ph/0003148].
- [36] P. Minkowski and W. Ochs, Phys. Lett. B **485** (2000) 139 [hep-ph/0003125].
- [37] G. Abbiendi *et al.* [OPAL], Eur. Phys. J. C **17** (2000) 373 [hep-ex/0007017].
- [38] R. Barate *et al.* [ALEPH], Eur. Phys. J. C **16** (2000) 613.
- [39] M. Acciarri *et al.* [L3], Phys. Lett. B **371** (1996) 126.
- [40] M. Acciarri *et al.* [L3], Phys. Lett. B **407** (1997) 389 Errat: [Phys. Lett. B **427** (1998) 409].
- [41] P. Abreu *et al.* [DELPHI], Phys. Lett. B **401** (1997) 118.
- [42] P. Abreu *et al.* [DELPHI], Eur. Phys. J. C **17** (2000) 207 [hep-ex/0106063].
- [43] R. A. Briere *et al.* [CLEO], Phys. Rev. D **76** (2007) 012005 [[arXiv:0704.2766 \[hep-ex\]](https://arxiv.org/abs/0704.2766)].
- [44] B. Andersson, “The Lund model,” Camb. Monogr. Part. Phys. Nucl. Phys. Cosmol. **7** (1997).
- [45] L. Lonnblad, Comput. Phys. Commun. **71** (1992) 15.
- [46] S. Schael *et al.* [ALEPH], Eur. Phys. J. C **48** (2006) 685 [hep-ex/0604042].
- [47] J. Abdallah *et al.* [DELPHI], Phys. Lett. B **643** (2006) 147 [hep-ex/0610031].
- [48] G. Rudolph, ”ALEPH results on quark and gluon fragmentation”, talk in workshop on parton fragmentation processes: in the vacuum and in the medium, ECT Trento. 2008.